Desalination and Water Treatment
www.deswater.com

doi: 10.1080/19443994.2015.1046150

57 (2016) 11904–11916
May

Taylor & Francis
Taylor & Francis Group

Preparation, characterization, and evaluation of *Moringa oleifera* pod husk adsorbents for aqueous phase removal of norfloxacin

Raymond A. Wuana*, Rufus Sha'Ato, Shiana Iorhen

Department of Chemistry and Centre for Agrochemical Technology, Federal University of Agriculture, Makurdi 970001, Nigeria, Tel. +2348066645047; email: raywuana@yahoo.com (R.A. Wuana)

Received 13 January 2015; Accepted 20 April 2015

ABSTRACT

Chemically treated and carbonized adsorbents were prepared from *Moringa oleifera* pod husks (MPH) and evaluated for the aqueous phase removal of Norfloxacin (NOX), a common antibiotic. The pulverized precursor was steeped in a saturated ammonium chloride solution (24 h) to give the chemically treated adsorbent (AMPH). Pyrolysis of AMPH (623 K, ½ h) yielded the carbonized adsorbent (CMPH). Both adsorbents showed favorable physicochemical attributes (pH, bulk density, attrition, iodine adsorption number/surface area, titratable surface charge, and FT-IR analysis). NOX removal was studied under the effects of initial solution pH (2–11), adsorbent dosage (0.5–2.5 g), initial NOX concentration (5–25 mg/L), contact time (0–240 min), and temperature (298–328 K). Optimal NOX uptake (mg/g) by AMPH (1.42) and CMPH (1.88) occurred at solution pH 5 and adsorbent dose of 0.5 g. Equilibrium adsorption obeyed the Langmuir isotherm. Free energy change (ΔG°), enthalpy change (ΔH°), and entropy change (ΔS°) indicated that the adsorption of NOX was feasible, spontaneous, exothermic, and physisorptive. Kinetically, NOX uptake increased rapidly within the first 10 min for both adsorbents and overall, was well modeled by the Blanchard pseudo-second-order equation. The adsorbents may find use in the removal of microcontaminants of pharmaceutical origin from effluents/wastewater.

Keywords: Norfloxacin; *Moringa oleifera* pod husks; Adsorption isotherms; Adsorption kinetics; Wastewater remediation

1. Introduction

Pharmaceuticals have been historically used to prevent or treat human, animal, and plant diseases. The global market for pharmaceuticals has been estimated between 100,000 and 200,000 ton/year [1] suggesting that pharmaceutical industries may be major sources of pharmaceutical waste in the environment [2,3]. It's no wonder then, that pharmaceuticals and personal care products are today, frequently listed among the most important emerging contaminants of concern in the environment [4–6]. Surface and groundwater contamination by pharmaceuticals such as analgesics, anti-depressants, contraceptives, and antibiotics has become an environmental issue of widespread concern [7]. In developing countries including Nigeria, one of the challenges faced by the pharmaceutical industry is the issue of pharmaceutical waste and its impact on the environment and public health owing to an improper healthcare waste management policy and plan [8,9].

*Corresponding author.

Antibiotics are probably the most successful pharmaceuticals so far developed to improve human health and for preventing and treating animal and plants infection as well as for promoting growth in animal farming and these applications lead to the release of large quantities of antibiotics to natural ecosystems [7,10,11]. The newest class of antibiotics, the fluoroquinolones (e.g. ciprofloxacin, levofloxacin, lomefloxacin, norfloxacin (NOX), sparfloxacin, clinafloxacin, gatifloxacin, ofloxacin, and trovafloxacin) are of great concern because they are most widely produced and used the world over and are not completely metabolized by the body. About 20–90% of fluoroquinolones ingested are excreted in their pharmacologically active forms, leading to significant loads being discharged into domestic sewage [12]. NOX is a fluoroquinolone that is active against a broad spectrum of gram-positive and gram-negative aerobic bacteria and has been linked to serious side effects which include ruptured tendons and neurological damage resulting from seizures. Studies show that within 24 h of drug administration, 26–32% of the administered dose is recovered in the urine as NOX with an additional 5–8% being recovered in the urine as six metabolites of considerably less antimicrobial potency. Facal recovery accounts for another 30% of the administered dose. This represents the unabsorbed drug along with a small contribution through biliary excretion [13].

In the aquatic environment, antibiotics may persist as microcontaminants and eventually be transported to reservoirs, surface, and groundwater sources which supply raw water to treatment plants [14]. Furthermore, these drugs cause unpleasant odors and skin disorders, microbial resistance among pathogen organisms or the death of microorganisms which are effective in wastewater treatment [15]. The resistant bacteria may also cause diseases that cannot be treated by conventional antibiotics [16].

Among the techniques for removal of contaminants, including pharmaceuticals from aqueous media, approaches involving adsorption on activated carbon are commonly used due to their high efficiency and easy applicability [17]. The superlative attributes of activated carbon such as large surface area, high porosity, controllable pore structure, thermal stability, and low acid–base reactivity have qualified it as a good adsorbent [18,19]. Those favorable attributes notwithstanding, the high cost and difficulties associated with regeneration of activated carbons have hampered their industrial applications. The need to circumvent this challenge has necessitated the quest for alternative adsorbents from cheaply available natural, renewable, and biomass-based precursors in water/wastewater remediation processes through research and development [20]. The potential of adsorbents from biomass such as saw dust [7], chestnut shell [21], cork [22], bamboo [23,24], and vine wood [25] to remove various pharmaceuticals or their intermediates from aqueous media have been previously reported. Consequently, the specific objectives of the present study were to prepare, characterize, and evaluate the effectiveness of adsorbents from *Moringa oleifera* pod husks (MPH) (biomass) to remove NOX, a common antibiotic from aqueous phase, with emphasis on adsorption equilibria, thermodynamics, and kinetics.

2. Experimental

2.1. Preparation and characterization of M. oleifera pod husk adsorbents

MPH were collected from stands in urban Makurdi (7.44°N 8.33°E), Nigeria, air-dried, pulverized using mortar/pestle, and the resulting powder sieved (<2 mm). The sieved material was chemically treated by steeping it in a saturated ammonium chloride (BDH Chemicals, 99%) solution for 1 d [26]. The slurry was filtered and the residue rinsed repeatedly with distilled water and air-dried to serve as the chemically (ammonium chloride) treated adsorbent (AMPH). A portion of AMPH was pyrolyzed in a muffle furnace (NEY M-525, USA) at 623 K for ½ h. The resulting carbon was washed repeatedly with distilled water to remove ash, air-dried, and stored as the carbonized adsorbent (CMPH).

The adsorbents were further characterized physicochemically. Adsorbent pH was determined by dispersing 1.0 g triplicate samples of the adsorbent in distilled water for 1 h and measuring the pH of the resulting filtrate [27]. Bulk density was determined by the tamping procedure of Ahmedna et al. [28]. Attrition was determined by a procedure described by Toles et al. [29]. Adsorbent surface area was determined by the iodine adsorption number method during which, a 0.5 g portion of the adsorbent was treated with an excess of standard iodine solution followed by back-titration of the unreacted iodine with standard sodium thiosulphate solution [26]. A blank titration was also performed on an aliquot of iodine solution not treated with the adsorbent. The iodine number, n_{I_2} (i.e. amount in moles of iodine adsorbed per g adsorbent) was calculated using Eq. (1); while the adsorbent surface area, A (m^2/g) was calculated with the aid of Eq. (2), a modified form of that of Shoemaker et al. [30]:

$$n_{I_2}(\text{mol/g}) = \frac{C_T(V_B - V_S)}{2 \times 10^3 m_{AD}} \quad (1)$$

$$A\ (\text{m}^2/\text{g}) = N_o n_{I_2} \sigma_{I_2} \quad (2)$$

where C_T is the concentration of the thiosulphate (mol/L), V_B and V_S are, respectively, the titer values of the blank and adsorbent-treated iodine solutions (L); m_{AD} is mass of the adsorbent used (0.5 g); N_o is the Avogadro's number; and σ_{I_2} is the cross-sectional area of an iodine molecule (m^2), given as 3.2×10^{-19} m^2. Titratable surface charge was determined by the Boehm titrimetric method described by Van Winkle [31]. Fourier transform infrared analysis utilized the FT-IR-8400s Shimadzu, Japan spectrophotometer, and was performed according to the manufacturer's specifications.

2.2. Preparation of calibration curve for UV–vis spectrophotometric determination of NOX

NOX ($C_{16}H_{18}FN_3O_3$; MW = 319.33 g/mol) was supplied by Ranbaxy Laboratories Limited (see Fig. 1 for chemical structure).

A 400 mg/L stock aqueous solution of NOX was prepared. Standard working concentrations: 5, 10, 15, 20, 25, 30, 40, 50, 60, 80, and 100 mg/L were obtained by serial dilution of appropriate volumes of the stock. Each dilution was measured in a UV–vis spectrophotometer (Surgispec SM 7525) at the wavelength where NOX absorbed the highest amount of UV radiation (λ_{max} = 274 nm). The absorbances were read and the linearity range of 5–25 mg/L obtained and used for constructing the calibration curve. The calibration curve was constructed so that the absorbance results collected through experimentation could be directly converted into concentration by extrapolating through the linearity range. The absorbance values were then plotted against the known concentrations of the standard solutions (Fig. 2). Actual NOX concentrations in experimental samples were calculated in accordance with Beer's Law.

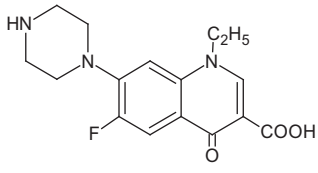

Fig. 1. Chemical structure of NOX (1-ethyl-6-fluoro1,4-dihydro-4-oxo-7-(1-piperazinyl)-3-quinoline carboxylic acid).

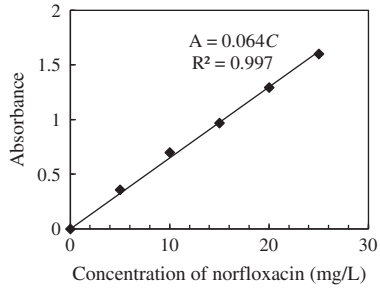

Fig. 2. Calibration curve for UV–vis spectrophotometric determination of NOX in aqueous solution (λ_{max} = 274 nm).

2.3. Adsorption experiments

Batch adsorption experiments were designed to assess the effect of various operational parameters (initial solution pH, adsorbent dose, contact time, temperature) on aqueous phase removal of NOX by AMPH and CMPH. Prior to this, the chemical stability of NOX was checked at 298 K, wherein separate aliquots (50 mL) of NOX standards (5, 15, and 25 mg/L) with or without treatment with 0.5 g AMPH or CMPH were kept for 0, 12, 24, 48, and 72 h followed by determination of the residual NOX concentrations by UV–vis spectrophotometry. NOX recoveries ranged from 95.20 to 103.30%. Since these were within the 70–130% accuracy range specified by guidelines [32] as acceptable, it was possible to confirm that the standard solutions and adsorbent-treated samples were stable for three consecutive days at 298 K. Consequently, a maximum NOX-adsorbent contact time of 4 h was chosen for this study to minimize possible antibiotic loss especially at the higher temperatures (308–328 K) investigated.

In order to study the effect of initial solution pH on adsorption of NOX, separate 50 mL aliquots of NOX solution (25 mg/L) were adjusted to pH 2, 5, 7, 9, and 11 by drop-wise addition of 0.1 M NaOH or 0.1 M HCl, as the case may be, with the aid of a pre-calibrated pH meter (HI96107, Hanna Instruments). The solutions were further contacted with 0.5 g of AMPH or CMPH adsorbents for 4 h with the aid of a mechanical shaker (HY-2, Jiangsu, China). The slurries were filtered and the residual NOX concentrations in the filtrate determined using the UV–vis spectrophotometer at 274 nm.

The effect of adsorbent dose on adsorption of NOX was investigated by dispersing accurately weighed portions (0.5, 1.0, 1.5, 2.0, and 2.5 g) of AMPH or CMPH in 50 mL aliquots of NOX (25 mg/L) solution with the aid of a mechanical shaker for 4 h. The

resulting slurries were filtered and the residual NOX concentrations in the filtrates measured using UV–vis spectrophotometer.

The effect of initial NOX solution concentration (adsorption isotherms) and temperature (adsorption thermodynamics) on adsorption process was studied by contacting 0.5 g of AMPH or CMPH with separate 50 mL portions of each of the NOX solutions prepared to furnish different initial concentrations, C_i in the range $5 \leq C_i$ (mg/L) ≤25 for 4 h on a thermostatic water bath (DINI2877-KI) at four different temperatures (298, 308, 318, and 328 K). The slurries were filtered and the residual NOX concentrations in the filtrates determined using UV–vis spectrophotometer.

Lastly, the effect of contact time (adsorption kinetics) on adsorption of NOX was assessed by contacting 0.5 g portions of AMPH or CMPH with separate 50 mL aliquots of 25 mg/L NOX solution for 10, 30, 60, 120, 180, and 240 min at 298 K on a thermostatic water bath. At the elapse of each specified time interval, the slurries were filtered and the residual NOX concentrations in the filtrate measured by UV–vis spectrophotometry. The procedure was repeated at 308, 318, and 328 K to study the effect of temperature of adsorption kinetics.

In all batch adsorption experiments, the amount of NOX adsorbed, Q (mg/g), was calculated by the mass balance equation:

$$Q(\text{mg/g}) = \frac{(C_i - C_f)V}{m_{AD}} \quad (3)$$

where C_i and C_f are the initial and final (residual) NOX concentrations (mg/L), respectively; V is the aliquot of NOX solution used (50 mL = 0.05 L); and m_{AD} is the mass of adsorbent (g) used for a particular batch treatment.

The percentage removal of NOX by AMPH and CMPH was calculated as:

$$\%\ \text{Removal} = \frac{(C_i - C_f)}{C_i} \times 100 \quad (4)$$

Quality control/assurance was achieved by good laboratory practices. All glassware and plastics were properly washed with acid (1 + 1 HNO_3) and finally with distilled water and oven-dried. Procedural blank samples were subjected to similar treatments using the same amounts of reagents. In all cases, measurements were done in triplicate.

3. Results and discussion

3.1. Physicochemical attributes of M. oleifera pod husk adsorbents

The physicochemical attributes of *M. oleifera* pod husks adsorbents (i.e. AMPH and CMPH) are recorded in Table 1. AMPH and CMPH had pH of 6.4 and 7.1, respectively. Adsorbents with pH 6–8 are acceptable for applicability for water and wastewater treatment [33]. Bulk densities of 105 and 178 kg/m^3, respectively, were recorded for AMPH and CMPH. AMPH and CMPH showed 9.39 and 12.55% attrition, respectively, somewhat higher than adsorbents from banana empty fruit bunch and *Delonix regia* fruit pod [34].

Attrition measures the adsorbent's ability to withstand frictional forces by stirring and washing and is an important parameter in understanding loss of adsorbent during handling and regeneration. Attrition values recorded in this study indicate that CMPH possesses a higher resistance to abrasion than AMPH. Iodine numbers (mg/g) and surface areas (m^2/g), respectively, were 256.40 and 182.41 for AMPH; 310.60 and 235.79 for CMPH, indicating higher values compared with those reported for *Hemidesmus indicus* [35], base-treated and carbonized rice husks [27], banana empty fruit bunch, and *D. regia* fruit pod [34]. Adsorbents with high iodine number/surface area perform better in the removal of small sized contaminants.

The titratable surface charge (mmol H^+eq/g) gives an indication of the acidic and basic functional groups on the adsorbent's surface. The titratable surface acidic groups were determined by selective neutralization with a series of bases of varying strength: $NaHCO_3$,

Table 1
Selected physicochemical attributes of *M. oleifera* pod husk adsorbents[a]

Attribute	AMPH	CMPH
pH_{water}	6.4	7.1
Bulk density (kg/m^3)	105.0	178.0
Attrition (%)	9.4	12.6
Iodine number (×10^{-3} mol/g)	1.0	1.2
Iodine number (mg/g)	256.4	310.6
Surface area (m^2/g)	182.4	235.8
Total surface charge (mmol H^+eq/g)		
NaOH	0.87	0.75
$NaHCO_3$	1.03	0.99
Na_2CO_3	0.87	0.61

[a]AMPH = ammonium chloride-treated *M. oleifera* pod husks and CMPH = carbonized *M. oleifera* pod husks.

Na_2CO_3 and NaOH whereby, $NaHCO_3$ neutralizes carboxylic groups (strong acidic groups), those neutralized by Na_2CO_3 but not by $NaHCO_3$ are lactones (weak acidic groups). The weak acid groups neutralized by NaOH but not by Na_2CO_3 were postulated as phenols (very weak acidic groups [36,37]. The order of the acidic groups on the surface of AMPH was carboxylic > lactones ≈ phenolic; while that for CMPH was carboxylic > phenolic > lactones. Aside the aforementioned groups, other oxygen-based acidic functional groups which may be present on the adsorbent's surface include quinine-type carbonyls, anhydrides, ethers, and cyclic peroxides [36,38].

FT-IR analysis helps in the identification of individual surface functional groups which could play a great role in adsorption mechanism and capacity. FT-IR spectra of the experimental adsorbents are presented in Fig. 3. AMPH shows a broad peak at 3,412/cm (2,500–3,500/cm) attributable to O–H stretch and N–H asymmetric stretching vibrations which could be due to inter and intramolecular hydrogen bonding. The band at 1,736.96/cm could be ascribed to C=O stretching vibrations indicating presence of aldehydic groups. The band at 1,645/cm could be attributed to C=C stretching of alkenes while that observed at 1,045/cm is ascribed to C–O stretching vibration of alcohols [39]. The CMPH spectrum shows similarities to that of AMPH with slight frequency shifts. Overall, the FT-IR frequency shifts indicate that NOX was bound to the adsorbents via hydroxyl, amine, carboxylic, hydrogen bonding, and aldehydic groups.

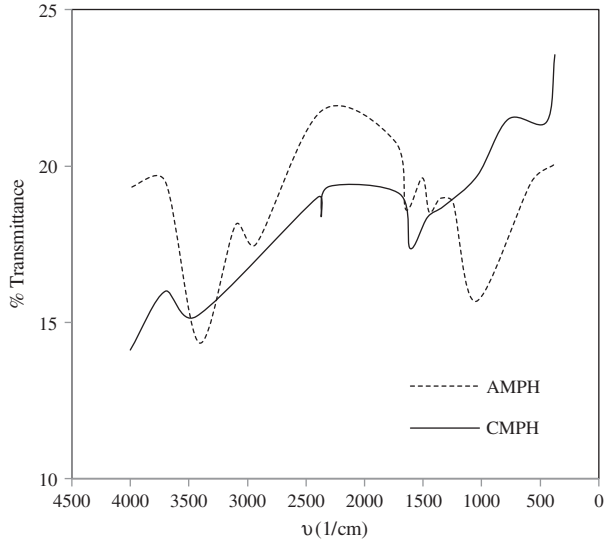

Fig. 3. Fourier transform infrared (FT-IR) spectra of ammonium chloride-treated (AMPH) and carbonized (CMPH) *M. oleifera* pod husks.

3.2. Effect of initial solution pH on aqueous phase removal of NOX

Fig. 4 illustrates the effect of initial solution pH on the aqueous phase sorptive removal of NOX by AMPH and CMPH. The adsorption capacity is influenced most by the pH of the solution since solution pH affects adsorbent's charge, degree of ionization, and chemical speciation of the adsorbate [22]. At pH 2, NOX uptake was 0.04 and 0.72 mg/g for AMPH and CMPH, respectively. As the pH was increased to 5, however, maximum uptake of 1.19 and 1.84 mg/g were achieved for AMPH and CMPH, respectively, an observation which may be attributed to hydrogen bonding between NOX and adsorbents [40,41]. A similar result was obtained by Punyapalakul and Sithisorn [42] who showed that the optimum pH for adsorption of ciprofloxacin onto functionalized silicates is 5. Percent removal was found to decrease slightly with increase in pH from 5 to 9. These results are also in agreement with those obtained by Bajpai et al. [7] who showed that the optimum pH for sorptive removal of ciprofloxacin using sawdust was 5.8. There was, however, a remarkable decrease in NOX uptake at pH 11 for AMPH (0.13 mg/g) and CMPH (0.65 mg/g). The somewhat linear decrease in the percent removal of NOX between pH 5–9 is noteworthy and may be due to the zwitterionic properties of NOX. The range of pK_a values of the NOX is 5.00–8.45. In acidic medium (low pH), NOX is positively charged. The adsorbents, on the other hand, possess a net negative structural charge at low pH and this favors adsorption [22,43]. At pH 5, high ionic interactions occur between the cationic NOX and AMPH or CMPH surface furnishing a high removal of NOX. At pH 7, where the dominant solution phase species is the zwitterion, a cationic state can still be accepted as a major contributor to sorption since a

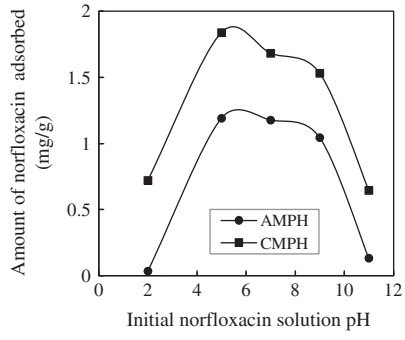

Fig. 4. Effect of initial solution pH on aqueous phase removal of NOX on ammonium chloride-treated (AMPH) and carbonized (CMPH) *M. oleifera* pod husks.

considerable amount of NOX was removed from the solution. At pH 9, the anionic state of NOX leads to a significant decrease in removal efficiency [44]. The very low and outlying removal efficiencies at pH 2 and 11 are possibly due to the alteration of the physicochemical properties of AMPH and CMPH at these extreme pH values [22].

3.3. Effect of adsorbent dosage on aqueous phase removal of NOX

The effect of AMPH and CMPH dosage on NOX removal is illustrated in Fig. 5(a) and (b). NOX uptake per unit mass of adsorbent decreased with increase in adsorbent dosage (0.5–2.5 g) for both AMPH and CMPH. This trend may be explained on the basis of the mass balance relationship (Eq. (3)). At increasingly higher adsorbent dosages, fixed initial solution concentration (25 mg/L), and fixed volume (50 mL), the available NOX molecules are not able to cover all the exchangeable sites on the adsorbents, resulting in low NOX uptake [45]. Maximum NOX uptake was 1.42 mg/g and 1.88 mg/g for AMPH and CMPH, respectively. Conversely, NOX removal efficiencies expressed as a function of only the initial and final NOX concentration (Eq. (4)) increased with increase in adsorbent dosage and ranged from 56.68 to 81.60% for AMPH and 75.28–90.68% for CMPH.

3.4. Equilibrium adsorption isotherm profiles and parameters

Equilibrium data from adsorption experiments are usually presented in the form of an isotherm, which graphically displays the ratio of adsorbed to non-sorbed solute per unit mass of the adsorbent at constant temperature. The isotherm profiles are important in providing information regarding the nature and mechanism of sorption for a particular adsorbate–adsorbent system. The isotherm profiles for the aqueous phase adsorption of NOX on AMPH and CMPH at the different temperatures are illustrated in Fig. 6.

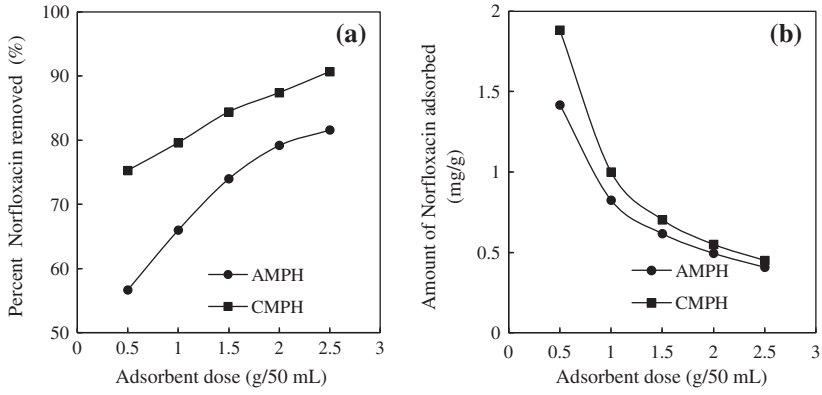

Fig. 5. Effect of adsorbent dosage on (a) percent of NOX removed and (b) amount of NOX adsorbed by ammonium chloride-treated (AMPH) and carbonized (CMPH) *M. oleifera* pod husks.

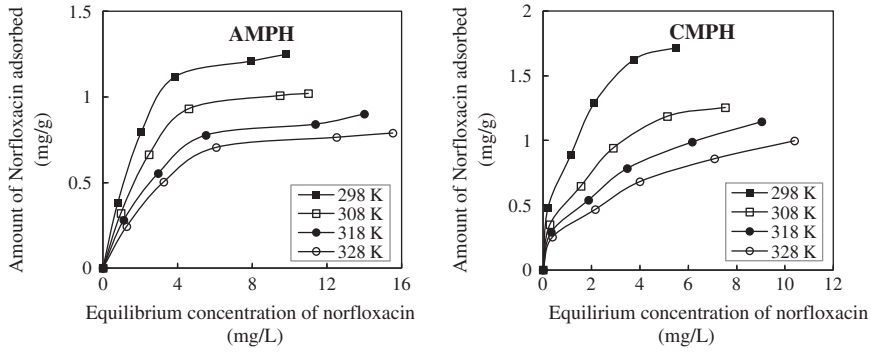

Fig. 6. Isotherm profiles for aqueous phase adsorption of NOX on ammonium chloride-treated (AMPH) and carbonized (CMPH) *M. oleifera* pod husks at different temperatures.

Consistent with Giles et al. [46] classification, the isotherms for AMPH and CMPH were somewhat L-shaped indicating that the intermolecular forces of NOX are comparatively weaker than the sorptive forces, which also implies that the activation energy of adsorption is independent of surface coverage.

Equilibrium data for the adsorption of NOX from aqueous phase on AMPH and CMPH were fitted into the linearized forms of the Langmuir (Eq. (5)) and Freundlich (Eq. (6)) models:

$$\frac{C_e}{Q_e} = \frac{C_e}{Q_{max}} + \frac{1}{K_L Q_{max}} \quad (5)$$

$$\ln Q_e = \frac{1}{n_F} \ln C_e + \ln K_F \quad (6)$$

where Q_e is the equilibrium amount of NOX adsorbed per unit mass of the adsorbent (mg/g), and C_e is the equilibrium (residual) concentration (mg/L). Q_{max} is the maximum amount of NOX adsorbed per unit mass of adsorbent (mg/g) corresponding to complete coverage of the adsorptive sites; K_L(L/mg) is the Langmuir constant related to the energy of adsorption. K_F is Freundlich constant ($mg^{1-1/n}L^{1/n}/g$), related to the adsorption capacity, and n_F is a dimensionless empirical parameter related to the adsorption intensity which varies with the heterogeneity of the material [47,48]. A linear plot of C_e/Q_e vs. C_e gives the inverse of the slope as Q_{max} and K_L is derived from the intercept; while a linear plot of ln Q_e vs. lnC_e gives the inverse of the slope as n_F and intercept as K_F. The Langmuir and Freundlich parameters are recorded in Table 2.

3.4.1. Langmuir isotherm parameters

The Langmuir model assumes that adsorption occurs at homogeneous sites and forms a monolayer. The characteristics of the Langmuir isotherm are determined by the dimensionless constant called the separation factor, R_L expressed as:

$$R_L = \frac{1}{(1 + K_L C_i)} \quad (7)$$

where K_L (L/mg) and C_i (mg/L) retain their meaning as earlier defined in Eqs. (3) and (5), respectively. R_L indicates the nature of adsorption process such that $R_L > 1$, $R_L = 1$, $0 < R_L < 1$, and $R_L = 0$ indicate that

Table 2
Isotherm parameters for aqueous phase adsorption of NOX on ammonium chloride-treated and carbonized *M. oleifera* pod husks at different temperatures[a]

Adsorbent	Isotherm parameters	298 K	308 K	318 K	328 K
AMPH	*Langmuir*				
	Q_{max} (mg/g)	1.517	1.255	1.035	0.967
	K_L (L/mg)	0.517	0.437	0.393	0.311
	K_L ($\times 10^5$ L/mol)	1.651	1.395	1.254	0.993
	R_L	0.070	0.080	0.090	0.110
	R^2	0.991	0.989	0.994	0.988
	Freundlich				
	K_F ($mg^{1-1/n}$ $L^{1/n}/g$)	0.498	0.379	0.314	0.239
	n_F	2.188	2.164	2.123	2.066
	R^2	0.897	0.898	0.835	0.891
CMPH	*Langmuir*				
	Q_{max} (mg/g)	2.033	1.490	1.366	1.064
	K_L (L/mg)	0.944	0.686	0.464	0.401
	K_L ($\times 10^5$ L/mol)	3.014	2.191	1.482	1.290
	R_L	0.041	0.060	0.080	0.090
	R^2	0.979	0.978	0.964	0.980
	Freundlich				
	K_F ($mg^{1-1/n}$ $L^{1/n}/g$)	0.904	0.609	0.451	0.367
	n_F	2.475	2.358	2.358	2.347
	R^2	0.988	0.936	0.991	0.995

[a]AMPH = ammonium chloride-treated *M. oleifera* pod husks and CMPH = carbonized *M. oleifera* pod husks.

adsorption is unfavorable, linear, favorable and irreversible, respectively [44].

Table 2 shows that at temperatures (298–328 K) considered in this study, the Langmuir parameters: Q_{max} (mg/g), K_L (L/mol) and R_L for the NOX-AMPH and NOX-CMPH systems decreased with increase in temperature, implying that the sorptive removal of NOX was favored less at elevated temperatures. Actual values of the Langmuir parameters were correspondingly higher for NOX-CMPH than the NOX-AMPH sorption system, qualifying CMPH as the more potent of the experimental adsorbents. The values of R_L are within the $0 \leq R_L \leq 1$ range representing favorable NOX adsorption for both adsorbents [44].

3.4.2. Freundlich isotherm

This Freundlich model proposes heterogeneous energetic distribution of active sites, accompanied by interaction between adsorbed molecules. Table 2 shows that at temperatures (298–328 K) considered in this study, the Freundlich parameters: K_F ($mg^{1-1/n}L^{1/n}/g$) and n_F for the NOX-AMPH and NOX-CMPH systems decreased with increase in temperature, indicating that the uptake of NOX was favored less at higher temperatures. The values of n_F ($2.475 \leq n_F \leq 2.066$) recorded in this study fall within the range $0 \leq n_F \leq 10$ and signify favorable NOX adsorption [44]. In magnitude, the Freundlich parameters were correspondingly higher for NOX-CMPH than the NOX-AMPH sorption system portraying CMPH as the more potent of the experimental adsorbents.

3.5. Thermodynamics of aqueous phase removal of NOX

Thermodynamic parameters such as Gibbs free energy change (ΔG°), enthalpy change (ΔH°), entropy (ΔS°) for adsorption of NOX on AMPH and CMPH were determined by manipulation of K_L values at different temperatures. The Gibbs free energy change was calculated using Eq. (8) [49]:

$$\Delta G^\circ = -RT \ln K_L \tag{8}$$

where R is the universal gas constant (8.314 J/mol K), T is the temperature (K). Meanwhile, the values of K_L, the Langmuir affinity constant, were first converted from L/mg basis to L/mol basis with the aid of Eq. (9) before substitution in Eq. (8):

$$K_L(\text{L/mol}) = K_L(\text{L/mg}) \times 10^3(\text{mg/g}) \times \text{MW}(\text{g/mol}) \tag{9}$$

where MW is the molecular weight of NOX (319.33 g/mol).

The enthalpy (ΔH°) and entropy (ΔS°) parameters were, respectively, estimated from the slope and intercept of the ln K_L(L/mol) vs. $1/T$ (1/K) plot according to the Van't Hoff equation:

$$\ln K_L = \frac{\Delta S^\circ}{R} - \frac{\Delta H^\circ}{RT} \tag{10}$$

where R and T retain their usual meanings as defined in Eq. (8).

The thermodynamic parameters: ΔG°; ΔH°, and ΔS° for aqueous phase adsorption of NOX on AMPH and CMPH are summarized in Table 3. Negative values of enthalpy change, ΔH° (kJ/mol), −13.20 and −23.92 for NOX-AMPH and NOX-CMPH sorption systems, respectively, can be ascribed to the exothermic nature of the adsorption process. In the literature, ΔH° values in the range [$-83 \leq \Delta H^\circ$ (kJ/mol) ≤ -830] represent chemisorption; while those in the range [$-8 \leq \Delta H^\circ$ (kJ/mol) ≤ -25] signify physisorption [50]. ΔH° values obtained in this study indicate that the adsorption of NOX on AMPH and CMPH occurred via physisorption. The positive values of entropy change, ΔS° (J/K mol), 5.66 and 24.44 for the NOX-AMPH and NOX-CMPH scenario, respectively, imply increase in the degree of disorder, hence the spontaneous nature of NOX adsorption on AMPH and CMPH. This further suggests that some changes occur in the internal structure of AMPH and CMPH during the adsorption process.

The negative values of Gibbs free energy, ΔG° (kJ/mol) for adsorption of NOX on both adsorbents ranging from [$-32.09 \leq \Delta G^\circ$ (kJ/mol) ≤ -29.77] indicate the feasibility of the adsorption process. From the literature, ΔG° values ranges from [$-20.00 \leq \Delta G^\circ$ (kJ/mol) ≤ 0.00] represent physisorption; while those in the range [$-400.00 \leq \Delta G^\circ$ (kJ/mol) ≤ -80.00] indicate chemisorptions [50]. The ΔG° values recorded in this study suggest the physisorptive mode of NOX removal.

3.6. Adsorption kinetics

Aside the adsorption capacity, derived from equilibrium considerations, the adsorption time (defined as the time taken to remove one-half of the initial concentration of the adsorbate) is another important parameter used to define an adsorbent for the selection of appropriate conditions for the design of a wastewater treatment scheme [51]. Rate curves for NOX-AMPH and NOX-CMPH sorption systems are

Table 3
Thermodynamic parameters of aqueous phase adsorption of NOX on ammonium chloride-treated and carbonized *M. oleifera* pod husks at different temperatures[a]

Adsorbent	T (K)	ΔG° (kJ/mol)	ΔH° (kJ/mol)	ΔS° (J/K mol)
AMPH	298	−29.766	−13.203	5.662
	308	−30.334		
	318	−31.039		
	328	−31.377		
CMPH	298	−31.257	−23.919	24.443
	308	−31.489		
	318	−31.478		
	328	−32.091		

[a]AMPH = ammonium chloride-treated *M. oleifera* pod husks and CMPH = carbonized *M. oleifera* pod husks.

illustrated in Fig. 7. For both adsorbents, NOX uptake increased very rapidly within the first 10 min, but slowed down beyond this point, gradually rendering plateaux at higher contact times for all the temperatures studied. By the 240th minute, the highest NOX uptake was 1.51 and 1.83 mg/g for AMPH and CMPH, respectively, signifying that the process would not offer additional kinetic advantage when contact times longer than 4 h were employed. The uptake of NOX, somewhat diminished as temperatures were raised from 298–328 K, implying that NOX adsorption was less favorable at higher temperatures.

The experimental data for the aqueous phase removal of NOX by AMPH and CMPH as a function of contact time were fitted into the Lagergren pseudo-first-order, LFOR (Eq. (11)), Blanchard pseudo-second-order, BSOR (Eq. (12)), and the Weber-Morris intraparticle diffusion, WMID (Eq. (13)) kinetic models [23,44,52–54]:

$$\ln(Q_e - Q_t) = \ln Q_e - k_1 t \tag{11}$$

$$\frac{t}{Q_t} = \frac{1}{k_2 Q_e^2} + \frac{t}{Q_e} \text{ (or) } \frac{t}{Q_t} = \frac{1}{h} + \frac{t}{Q_e} \tag{12}$$

$$Q_t = k_{id}\sqrt{t} + C \tag{13}$$

where Q_e and Q_t are, respectively, the amounts of NOX adsorbed (mg/g) at equilibrium and at a specified time, t (min); k_1 (/min), k_2 (g/mg min), and k_{id} (mg/g min$^{1/2}$) are the LFOR rate constant, BSOR rate constant, and WMID rate constant, respectively. In the BSOR model, the initial adsorption rate, h equals $k_2 Q_e^2$. Table 4 records the parameters rendered by the corresponding plots of ln (Q_e–Q_t) vs. t; $1/Q_t$ vs. t and Q_t vs. $\sqrt{t}$.

The order of magnitude of the kinetic parameters for the NOX-AMPH and NOX-CMPH sorption systems recorded across the temperatures varied in the sequence: $k_1(10^{-3}) < k_2\ (10^{-2}) \approx k_{id}\ (10^{-2})$. Values of k_1 did not reveal a regular trend with increase in temperature, possibly because the kinetic data was not well modeled by LFOR. For the BSOR model,

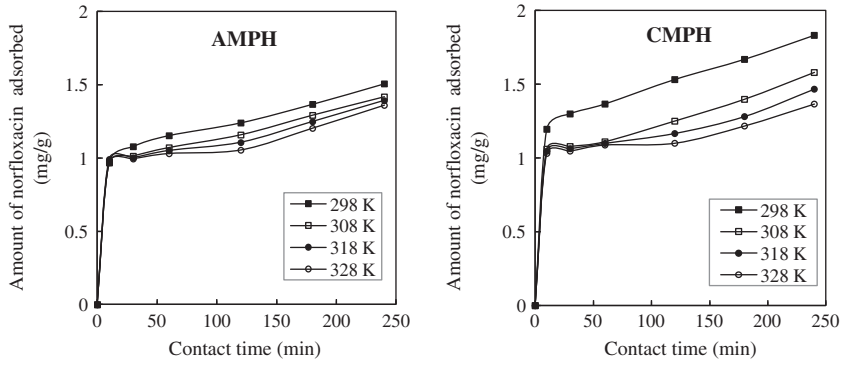

Fig. 7. Rate curves for aqueous phase adsorption of NOX on ammonium chloride-treated (AMPH) and carbonized (CMPH) *M. oleifera* pod husks at different temperatures.

Table 4
Kinetic parameters for aqueous phase removal of NOX by ammonium chloride-treated and carbonized *M. oleifera* pod husks at different temperatures[a]

Adsorbent	Model parameter	298 K	308 K	318 K	328 K
AMPH	*Lagergren*				
	k_1 ($\times 10^{-3}$/min)	7.0	7.0	6.0	7.0
	R^2	0.975	0.951	0.925	0.951
	Blanchard				
	Q_e (mg/g)				
	k_2 ($\times 10^{-2}$ g/mg min)	6.57	6.92	7.00	7.21
	R^2	0.988	0.987	0.984	0.981
	Weber-Morris				
	k_{id} ($\times 10^{-2}$ mg/g min^{½})	4.0	3.5	3.3	3.1
	C' (mg/g)	0.838	0.819	0.811	0.802
	R^2	0.979	0.955	0.921	0.877
CMPH	*Lagergren*				
	k_1 ($\times 10^{-3}$/min)	7.0	6.0	4.0	4.0
	R^2	0.986	0.939	0.941	0.866
	Blanchard				
	Q_e				
	k_2 ($\times 10^{-2}$ g/mg min)	5.22	5.24	6.93	9.00
	R^2	0.989	0.981	0.983	0.986
	Weber-Morris				
	k_{id} ($\times 10^{-2}$ mg/g min^{½})	5.0	4.1	3.1	2.4
	C' (mg/g)	1.012	0.856	0.891	0.913
	R^2	0.983	0.905	0.861	0.823

[a]AMPH = ammonium chloride-treated *M. oleifera* pod husks and CMPH = carbonized *M. oleifera* pod husks.

calculated Q_e, k_2, and h increased with increase in temperature, whereas k_{id} showed a converse trend for both adsorbents. Linear plots resulting from the WMID model did not pass through the origin suggesting that intra-particle diffusion was not the sole rate determining step in the sorption process [44,55]. Based on the coefficient of determination, R^2, the BSOR model recorded the highest values relative to LFOR and WMID. It, therefore, seemed that the adsorption kinetics was well interpreted by the BSOR model. Bajpai and Jain [56] also showed that at 300 K, the kinetic uptake of NOX ($C_i = 60$ and 100 mg/L) on spent tea leaves adsorbent was best interpreted by the BSOR. The k_2 values thereof, were of lower order of magnitude (10^{-4}) compared with those for NOX-AMPH and NOX-CMPH sorption systems.

4. Conclusion

The adsorbents prepared in this study showed favorable physicochemical attributes (pH, bulk density, attrition, iodine adsorption number/surface area, titratable surface charge, and FT-IR analysis). Chemical stability check showed that aqueous NOX solutions with or without AMPH and CMPH samples were stable for three days at 298 K. Batch sorption experiments conducted to investigate the effects of operating conditions such as initial NOX solution pH (2–11), adsorbent dosage (0.5–2.5 g), initial solution concentration (5–25 mg/L), contact time (0–240 min), and temperature (288–328 K) on NOX removal showed that at equilibrium, optimal NOX uptake (mg/g) occurred at pH 5 and sorbent dose of 0.5 g for both adsorbents. Langmuir isotherm described the equilibrium adsorption data better than the Freundlich model. The thermodynamic parameters indicated that the adsorption of NOX was feasible, spontaneous, exothermic, and physisorptive in nature. Rate studies revealed that the removal of NOX was very rapid within the first 10 min for both adsorbents, but slowed down beyond this point, implying that the process would not offer additional kinetic advantage when contact times longer than 4 h were employed. NOX uptake by both adsorbents, somewhat diminished as temperatures were raised from 298 to 328 K, implying that NOX removal was less favorable at elevated temperatures. The adsorption kinetic data was well represented by the Blanchard pseudo-second-order model. These adsorbents may find potential use in the removal of microcontaminants of pharmaceutical origin from effluents/wastewater.

Acknowledgments

Ms Shiana Iorhen gratefully appreciates the Heads of Department of Chemistry and Biochemistry, Benue State University, Makurdi for granting access to the laboratories. Mr Pius Utange of the Department of Chemistry, Benue State University, Makurdi, is also appreciated for his technical assistance.

List of symbols

A	—	adsorbent surface area (m^2/g)
n_{I_2}	—	amount in moles of iodine adsorbed per g adsorbent
σ_{I_2}	—	cross-sectional area of an iodine molecule (m^2)
ΔG°	—	Gibbs free energy change (kJ/mol)
ΔH°	—	enthalpy change (kJ/mol)
ΔS°	—	entropy change (J/K mol)
C_e, C_f	—	equilibrium, final (residual) concentration of NOX (mg/L)
C_i	—	initial NOX concentrations (mg/L), respectively
C_T	—	concentration of the thiosulphate (mol/L)
k_1	—	Lagergren pseudo-first-order rate constant (/min)
k_2	—	Blanchard pseudo-second-order rate constant (g/mg min)
K_F	—	Freundlich constant ($mg^{1-1/n}\,L^{1/n}/g$), related to the adsorption capacity
k_{id}	—	Weber-Morris intraparticle diffusion rate constant ($mg/g\,min^{1/2}$)
K_L	—	Langmuir constant related to the energy of adsorption (L/mg)
m_{AD}	—	mass of the adsorbent used for any batch experiment
MW	—	molecular weight of NOX (319.33 g/mol)
n_F	—	Freundlich dimensionless parameter related to the adsorption intensity
N_o	—	Avogadro's number (6.026×10^{23}/mol)
NOX	—	norfloxacin (an antibiotic of the fluoroquinolone class)
Q, Q_e, Q_t	—	amount of norfloxacin adsorbed (mg/g)
Q_{max}	—	maximum amount of NOX adsorbed per unit mass of adsorbent (mg/g)
R	—	universal gas constant (8.314 J/mol K)
R_L	—	Langmuir dimensionless separation factor
T	—	absolute temperature (K)
T	—	contact time between NOX and adsorbent (min)
V	—	aliquot of NOX solution used for a particular batch treatment
v	—	Infrared absorption frequency (1/cm)
V_B, V_S	—	titre values of the blank and adsorbent-treated iodine solutions (L)
λ_{max}	—	wavelength of maximum absorption of NOX (274 nm)

References

[1] E. Zuccato, S. Castiglioni, R. Bagnati, M. Melis, R. Fanelli, Source, occurrence and fate of antibiotics in the Italian aquatic environment, J. Hazard. Mater. 179 (2010) 1042–1048.
[2] D.G.J. Larsson, C. de Pedro, N. Paxeus, Effluent from drug manufactures contains extremely high levels of pharmaceuticals, J. Hazard. Mater. 148 (2007) 751–755.
[3] D. Li, M. Yang, J. Hu, Y. Zhang, H. Chang, F. Jin, Determination of penicillin G and its degradation products in a penicillin production wastewater treatment plant and the receiving river, Water Res. 42 (2008) 307–317.
[4] M. Mcbride, J. Wyckoff, Emerging liabilities from pharmaceuticals and personal care products, Environ. Claim. J. 14 (2002) 175–189.
[5] J. Fawell, C.N. Ong, Emerging contaminants and the implications for drinking water, Int. J. Water Resour. Dev. 28 (2012) 247–263.
[6] Q. Bu, Bin. Wang, J. Huang, S. Deng, G. Yu, Pharmaceuticals and personal care products in the aquatic environment in China: A review, J. Hazard. Mater. 262 (2013) 189–211.
[7] S.K. Bajpai, M. Bajpai, N. Rai, Sorptive removal of ciprofloxacin hydrochloride from simulated wastewater using sawdust: Kinetic study and effect of pH, Water SA 38 (2012) 673–682.
[8] N Ngwuluka, N. Ochekpe, P. Odumosu, S.A. John, Waste Management in Healthcare Establishments within Jos Metropolis, Nigeria, Afr. J. Environ. Sci. Technol. 3 (2009) 459–465.
[9] O.O. Fadipe, K.T. Oladepo, J.O. Jeje, M.O. Ogedengbe, Characterization and analysis of medical solid waste in Osun State, Nigeria, Afr. J. Environ. Sci. Technol. 5 (2011) 1027–1038.
[10] F.C. Cabello, Heavy use of prophylactic antibiotics in aquaculture: A growing problem for human and animal health and for the environment, Environ. Microbiol. 8 (2006) 1137–1144.
[11] J.L. Martinez, Environmental pollution by antibiotics and by antibiotic resistance determinants, Environ. Pollut. 157 (2009) 2893–2902.
[12] K. Kümmerer, Antibiotics in the aquatic environment —A review—Part I, Chemosphere 75 (2009) 417–434.
[13] P.C. Sharma, A. Saneja, S. Jain, Norfloxacin: A therapeutic review, Int. J. Chem. Sci. 6 (2008) 1702–1713.
[14] Z. Ye, H.S. Weinberg, M.T. Meyer, Occurrence of antibiotics in drinking water, Anal. Bioanal. Chem. 387 (2007) 1365–1377.
[15] S. Budyanto, S. Soedjono, W. Irawati, N. Indraswati, Studies of adsorption equilibria and kinetics of amoxicillin from simulated wastewater using activated carbon and natural bentonite, J. Environ. Protect. Sci. 2 (2008) 72–80.
[16] D.I. Anderson, Persistence of antibiotic resistant bacteria, Curr. Opin. Microbiol. 6 (2003) 489–493.
[17] H.E.M. El-Sayed, M.M.H. El-Sayed, Assessment of food processing and pharmaceutical industrial wastes as potential biosorbents: A review, BioMed Res. Int. (2014) 1–24.
[18] A.K. Bhattacharya, S.N. Mandal, S.K. Das, Adsorption of Zn(II) from aqueous solution by using different adsorbents, Chem. Eng. J. 123 (2006) 43–51.

[19] M. Grassi, G. Kaykioglu, V. Belgiorno, G. Lofrano, Removal of emerging contaminants from water and wastewater by adsorption process, in: G. Lofrano (Ed.), Emerging Compounds Removal from Wastewater, Springer Briefs in Green Chemistry for Sustainability, Springer, London, 2012, pp. 15–37, doi: 10.1007/978-94-007-3916-1_2
[20] D. Kalderis, D. Koutoulakis, P. Paraskeva, E. Diamadopoulos, E. Otal, J.O. Delvalle, C.P. Fernández, Adsorption of polluting substances on activated carbons prepared from rice husk and sugarcane bagasse, Chem. Eng. J. 144 (2008) 42–50.
[21] A. Sheikh Mohammadi, M. Sardar, The removal of penicillin G from aqueous solutions using chestnut shell modified with H_2SO_4: Isotherm and kinetic study, Iran J. Health Environ. 6 (2012) 497–508.
[22] M. Crespo-Alonso, V.N. Nurchi, R. Biesuz, G. Alberti, N. Spano, M.I. Pilo, G. Sanna, Biomass against emerging pollution in wastewater: Ability of cork for the removal of ofloxacin from aqueous solutions at different pH, J. Environ. Chem. Eng. 1 (2013) 1199–1204.
[23] G. Wu, X. Sun, H. Hui, X. Zhang, J. Yan, Q. Zhang, Adsorption of 2,4-dichlorophenol from aqueous solution by activated carbon derived from moso bamboo processing waste, Desalin. Water Treat. 51 (2013) 4603–4612.
[24] Y. Fan, B. Wang, S. Yuan, X. Wu, J. Chen, L. Wang, Adsorptive removal of chloramphenicol from wastewater by NaOH modified bamboo charcoal, Bioresour. Technol. 101 (2010) 7661–7664.
[25] H.R. Pouretedal, N. Sadegh, Effective removal of amoxicillin, cephalexin, tetracycline and penicillin G from aqueous solutions using activated carbon nanoparticles prepared from vine wood, J. Water Process Eng. 1 (2014) 64–73.
[26] F.E. Okieimen, C.O. Okieimen, R.A. Wuana, Preparation and characterization of activated carbon from rice husks, J. Chem. Soc. Niger. 32 (2007) 126–136.
[27] R.A. Wuana, L. Leke, D.A. Okibe, M. Okei, Aqueous phase adsorption of Cu(11) and Co(11) Ions from single and bisolute solutions onto base-treated and carbonized rice husks, Niger. J. Applied Sci. 27 (2009) 129–136.
[28] M. Ahmedna, W.E. Marshall, R.M. Rao, Production of granular activated carbons from selected agricultural by-products and evaluation of their physical, chemical and adsorption properties, Bioresour. Technol. 71 (2000) 113–123.
[29] C.A. Toles, W.E. Marshall, M.M. Johns, L.A. Wartelle, A. McAloon, Acid-activated carbons from almond shells: Physical, chemical and adsorptive properties and estimated cost of production, Bioresour. Technol. 71 (2000) 87–92.
[30] D.P. Shoemaker, C.W. Garland, J.W. Nibbler, Experiments in Physical Chemistry, Mc-Graw-Hill Publishing Company, New York, NY, 1989, p. 353.
[31] S.C. Van Winkle, The Effect of Activated Carbon on the Organic and Elemental Composition of Plant Tissue Culture Medium, PhD Dissertation, Institute of paper Science and Technology, Atlanta Georgia, 2000 p. 64.
[32] USDHHS-FDA, Guidance of Industry-Bioanalytical Method Validation, 2001, p. 5. Available from: <http://www.fda.gov/downloads/Drugs/Guidances/ucm070107.pdf–>
[33] F.E. Okiemen, F.I. Ojokoh, C.O.Okiemen, R.A.Wuana, Preparation and evaluation of activated carbon from rice husk and rubber seed shell, ChemClass J. (2004) 191–196.
[34] P. Sugumaran, V.P. Susan, P. Ravichandran, S. Seshadri, Production and characterization of activated carbon from banana empty fruit bunch and *Delonix regia* fruit pod, J. Sustainable Eng. Environ. 3 (2012) 125–132.
[35] V. Srihari, D. Ashutosh, Adsorption of phenol from aqueous media by an agro-waste *Hemidesmus indicus* based activated carbon, Appl. Ecol. Environ. Res. 7 (2009) 13–23.
[36] M.A.A. Akl, M.B. Dawy, A.A. Serage, Efficient removal of phenol from water samples using sugarcane bagasse based activated carbon, J. Anal. Bioanal. Technol. 5 (2014) 189–150.
[37] D.V. Bojić, M.S. Ranđelović, A.R. Zarubica, J.Z. Mitrović, M.D. Radović, M.M. Purenović, A.Lj. Bojić, Comparison of new biosorbents based on chemically modified *Lagenaria vulgaris* shell, Desalin. Water Treat. 51 (2013) 6871–6881.
[38] D.K. Mahmoud, M.A.M. Salleh, W.A.W. Abdul Karim, Characterization and evaluation agricultural solid wastes as adsorbents: A review, J. Purity Utility React. Environ. 1 (2012) 451–459.
[39] A.H. Sulaymon, D.W. Abbood, A.H. Ali, A comparative adsorption/biosorption for the removal of phenol and lead onto granular activated carbon and dried anaerobic sludge, Desalin. Water Treat. 51 (2013) 2055–2067.
[40] V.V. Goud, K.M. Mohanty, M.S. Rao, N.S. Jayakumar, Phenol removal from aqueous solutions by tamarind nutshell activated carbon: Batch and column studies, Chem. Eng. Technol. 28 (2005) 814–821.
[41] D. Tang, Z. Zheng, K. Lin, J. Luan, Adsorption of *p*-nitro phenol from aqueous solutions onto activated carbon fiber, J. Hazard. Mater. 143 (2007) 49–56.
[42] P. Punyapalakul, T. Sitthisorn, Removal of ciprofloxacin and carbamazepine by adsorption on functionalized mesoporous silicates, World Acad. Sci. Eng. Technol. 69 (2010) 546–550.
[43] C.E. Lin, Y.J. Deng, W.S. Liao, S.W. Sun, W.Y. Lin, C.C. Chen, Electrophoretic behavior and pK_a determination of quinolones with a piperazinyl substituent by capillary zone electrophoresis, J. Chromatogr. 2004 (1051) 283–290.
[44] M. Maheshwari, R.K. Vyas, M. Sharma, Kinetics, equilibrium and thermodynamics of ciprofloxacin hydrochloride removal by adsorption on coal fly ash and activated alumina, Desalin. Water Treat. (2013) 7241–7254.
[45] M. Moyo, E. Mutare, F. Chigondo, B.C. Nyamunda, Removal of phenol from aqueous solution by adsorption on yeast (*Saccharomyces cerevisiae*), Int. J. Res. Rev. Appl. Sci. 11 (2012) 486–494.
[46] C.H. Giles, D. Smith, A. Huitson, A general treatment and classification of the solute adsorption isotherm. I. Theoretical, J. Colloid Interface Sci. 47 (1974) 755–765.
[47] R.C. Bansal, M. Goyal, Activated Carbon Adsorption, Taylor and Francis Group, Boca Raton, FL, 2005, pp. 33487–33487.

[48] A. El-Maghraby, N.A. Taha, Equilibrium and kinetic studies for the removal of cationic dye using banana pith, Adv. Environ. Res. 3 (2014) 217–230.
[49] K.M. Doke, M. Yusufi, R.D. Joseph, E.M. Khan, Biosorption of hexavalent chromium onto wood apple shell: Equilibrium, kinetic and thermodynamic studies, Desalin. Water Treat. 50 (2012) 170–179.
[50] T. Dula, K. Siraj, S.A. Kitte, Adsorption of hexavalent chromium from aqueous solution using chemically activated carbon prepared from locally available waste of bamboo (*Oxytenanthera abyssinica*), ISRN, Environ. Chem. (2014) 1–10.
[51] W.E. Marshall, L.H. Wartelle, D.E. Boler, M.M. Johns, C.A. Toles, Enhanced metal adsorption by soybean hulls modified with citric acid, Bioresour. Technol. 69 (1999) 263–268.
[52] S.A. Patil, S.K. Patil, S.T. Salunkhe, S.S. Kolekar, Mahogany fruit shell: A new low-cost adsorbent for removal of methylene blue dye from aqueous solutions, Desalinat. Water Treat. 53 (2015) 99–108.
[53] S. Kaur, S. Rani, R.K. Mahajan, Adsorptive removal of dye crystal violet onto low-cost carbon produced from Eichhornia plant: kinetic, equilibrium, and thermodynamic studies, Desalin. Water Treat. 53 (2015) 543–556.
[54] P.S. Kumar, R. Sivaranjanee, U. Vinothini, M. Raghavi, K. Rajasekar, K. Ramakrishnan, Adsorption of dye onto raw and surface modified tamarind seeds: isotherms, process design, kinetics and mechanism, Desalin. Water Treat. 52 (2014) 2620–2633.
[55] B.K. Hamad, A.M. Noor, A.A. Rahim, Removal of 4-chloro-2-methoxyphenol from aqueous solution by adsorption to oil palm shell activated carbon activated with K_2CO_3, J. Phys. Sci. 22 (2011) 39–55.
[56] S.K. Bajpai, A. Jain, Dynamic uptake of drug norfloxacin from aqueous solution using spent tea leaves as a sorbent, Int. J. Environ. Waste Manage. 13 (2014) 376–395.